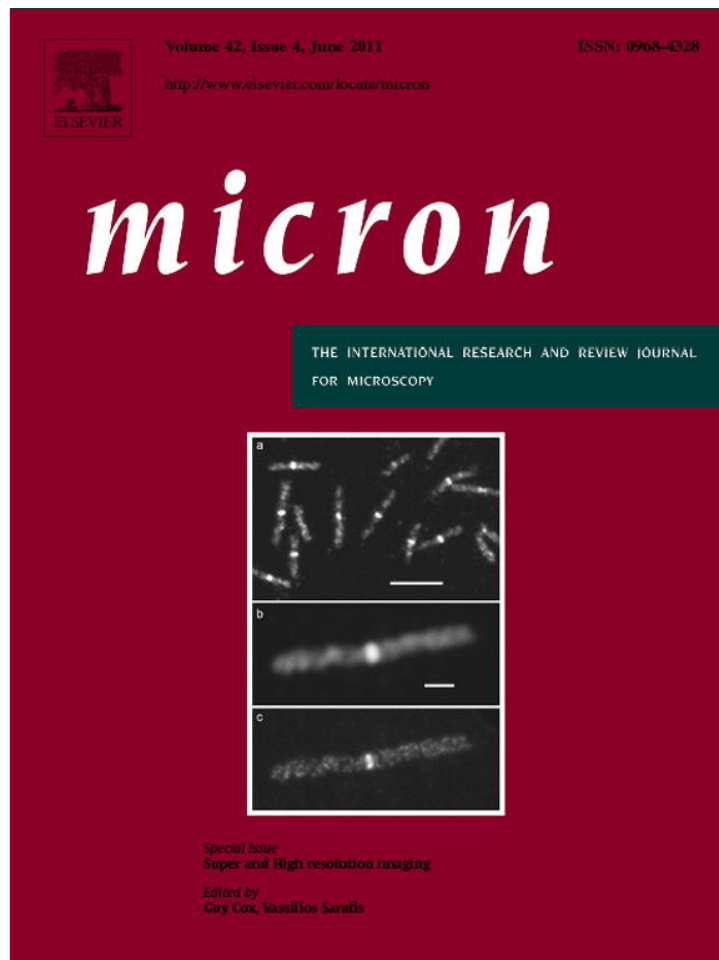


Provided for non-commercial research and education use.  
Not for reproduction, distribution or commercial use.



This article appeared in a journal published by Elsevier. The attached copy is furnished to the author for internal non-commercial research and education use, including for instruction at the authors institution and sharing with colleagues.

Other uses, including reproduction and distribution, or selling or licensing copies, or posting to personal, institutional or third party websites are prohibited.

In most cases authors are permitted to post their version of the article (e.g. in Word or Tex form) to their personal website or institutional repository. Authors requiring further information regarding Elsevier's archiving and manuscript policies are encouraged to visit:

<http://www.elsevier.com/copyright>



Contents lists available at ScienceDirect

Micron

journal homepage: [www.elsevier.com/locate/micron](http://www.elsevier.com/locate/micron)

## Structured illumination microscopy of autofluorescent aggregations in human tissue

Gerrit Best<sup>a</sup>, Roman Amberger<sup>a</sup>, David Baddeley<sup>a,b</sup>, Thomas Ach<sup>c</sup>, Stefan Dithmar<sup>c</sup>, Rainer Heintzmann<sup>d,e</sup>, Christoph Cremer<sup>a,f,g,\*</sup>

<sup>a</sup> Applied Optics and Information Processing, Kirchhoff-Institute for Physics, University of Heidelberg, Heidelberg, Germany

<sup>b</sup> Department of Physiology, Faculty of Medical and Health Sciences, University of Auckland, Auckland, New Zealand

<sup>c</sup> Department of Ophthalmology, University Hospital Heidelberg, Heidelberg, Germany

<sup>d</sup> Randall Division of Cell and Molecular Biophysics, King's College London, London, United Kingdom

<sup>e</sup> Institute of Photonic Technology, Jena, Germany

<sup>f</sup> Institute for Pharmacy and Molecular Biotechnology, University of Heidelberg, Heidelberg, Germany

<sup>g</sup> Institute for Molecular Biophysics, The Jackson Laboratory, Bar Harbor, Maine, USA

### ARTICLE INFO

#### Article history:

Received 10 February 2010

Received in revised form 16 June 2010

Accepted 17 June 2010

#### Keywords:

Structured illumination

Microscopy

Autofluorescence

Retinal pigment epithelium

Interferometer

### ABSTRACT

Sections from human eye tissue were analyzed with Structured Illumination Microscopy (SIM) using a specially designed microscope setup. In this microscope the structured illumination was generated with a Twyman-Green Interferometer. This SIM technique allowed us to acquire light-optical images of autofluorophore distributions in the tissue with previously unmatched optical resolution. In this work the unique setup of the microscope made possible the application of SIM with three different excitation wavelengths (488, 568 and 647 nm), thus enabling us to gather spectral information about the autofluorescence signal.

© 2010 Elsevier Ltd. All rights reserved.

### 1. Introduction

Compared to other microscopy methods used in biomedical research, fluorescence microscopy has several advantages in terms of sample preparation as well as the variety of possibilities to extract biologically significant information. A major problem, however, of any standard fluorescence microscopy method compared to non-light-optical microscopy methods remains the intrinsically limited conventional resolution of about 200 nm (Abbe, 1873; Rayleigh, 1896). Over the last years different techniques referred to as super resolution fluorescence microscopy have been established to compensate for this deficiency. These techniques (i.e. 4Pi (Cremer and Cremer, 1978; Hell and Stelzer, 1992), STED (Hell and Wichmann, 1994), SIM/PEM (Gustafsson, 2000; Heintzmann and Cremer, 1999) and localization methods (Cremer et al., 2010)), are based on conditions not considered in the original contributions of Abbe and Rayleigh. In combination with novel optoelectrical and mathematical tools, these different approaches have allowed the microscope to surpass the conventional resolution limit sub-

stantially, both in the object plane and in the direction along the optical axis of the microscope system.

In this report the method of Structured Illumination Microscopy (SIM), also referred to as patterned excitation microscopy (PEM), was applied to the investigation of the retinal pigment epithelium (RPE) in human eye tissue samples. SIM utilizes, in contrast to standard widefield (non-scanning) fluorescence microscopy, a periodically modulated excitation intensity in the object plane.

The RPE, which supports the functioning of the retina, is a cell monolayer between the rod outer segments and the Bruch's membrane. Age-related macular degeneration is primarily caused by a degeneration of the RPE. This degeneration is accompanied by excessive aggregations of lipofuscin. Lipofuscin consists of a variety of fluorescent and non-fluorescent proteins (Eldred and Katz, 1988) and lipids (Ng et al., 2008), and is mostly contained in the lysosomal residual bodies forming lipofuscin granules.

Lipofuscin exhibits autofluorescence across the visual spectrum (Sparrow et al., 2000), making fluorescence microscopy an attractive method to investigate the deposits of these pigments. Structured illumination imaging at three different wavelengths (488, 568, 647 nm) has allowed us to study the distribution of lipofuscin at a level of detail inaccessible to conventional fluorescence microscopy and to attain additional spectral information about the aggregations.

\* Corresponding author at: Applied Optics and Information Processing, Kirchhoff-Institute for Physics, University of Heidelberg, Heidelberg, Germany.

E-mail address: [cremer@kip.uni-heidelberg.de](mailto:cremer@kip.uni-heidelberg.de) (C. Cremer).

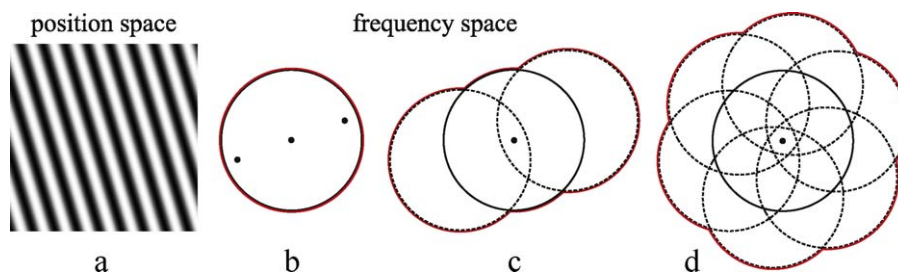


**Fig. 1.** Extension of the accessible frequency region by SIM. The sinusoidal illumination pattern (a) contains three delta-peaks in frequency space as illustrated in the Fourier transformed raw image (b). The red outline demonstrates the frequency limit. The raw data (b) consists of superposed original image information positioned at three different origins. After separation, the information can be shifted back to its respective position resulting in an expanded accessible frequency area (c). To expand the resolution in the object plane isotropically, the illumination is rotated (d).

## 2. Methods

### 2.1. Structured illumination microscopy

#### 2.1.1. Principle of SIM

In conventional microscopy, the optical resolution is constrained by the wavelength of the detected light to approximately 200 nm.

Although this limit is a universal principle that cannot be broken directly, SIM is able to code high resolution information into the low resolution supported region of the microscope and thus circumvent the limit. The required conditions are generated in SIM by illuminating the object with a periodic pattern (e.g. a sine squared as described by Heintzmann and Cremer (1999) and Gustafsson (2000)).

The effect of this process in the image plane is visualized in Fig. 1: The object is illuminated with a sine square intensity pattern (a). By this operation in position space (multiplication of the object distribution with a sine square), in Fourier Space (b) the object's spatial frequencies are shifted by the spatial frequencies  $\nu_x = 1/P_x$ ,  $\nu_y = 1/P_y$  with the period of the sine square in  $x$  and  $y$  direction  $P_x$  and  $P_y$ . In total thereby three copies of the original Fourier-transformed object are generated. Two copies are originated at the negative and the positive grating frequency, while a central copy stays originated at the zero spatial frequency. The three copies exist jointly in the Fourier-transformed image (b). As the high spatial frequencies are cut off by the objective (the cut-off frequency is illustrated by the red circle in (b)) object information of high frequency that usually would lie outside the supported region ( $\nu > \nu_{\max}$ ) is coded in the transmittable frequency region.

An acquisition of a series of images with the grating at different positions makes it possible to identify the shifted information afterwards and transfer it back to its proper frequency position (Fig. 1c). This procedure results in a broadened support region in frequency space and thereby in an improvement of optical resolution in the direction of the modulation of the illumination pattern. To achieve an isotropic resolution in the lateral (object) plane, the direction of modulation of the excitation intensity has to be changed (i.e. the illumination pattern has to be rotated). Here the illumination pattern is rotated by  $60^\circ$  subsequently to three different acquisition orientations, which results in an accessible frequency domain of a shape as indicated in Fig. 1d and a sufficiently isotropic resolution improvement.

Since the illumination pattern is projected into the object plane through the objective lens, the spatial frequencies of the pattern have to be smaller than the cut-off frequency of the objective lens for the excitation wavelength. As the excitation wavelength is usually close to the fluorescence emission wavelength, the excitation cut-off frequency is close to the accordant frequency for the emission light. Because of these facts, the maximal resolution

improvement that can be achieved with linear SIM is roughly by a factor of two.

The theory behind linear structured illumination resolution improvement has been described in detail by Heintzmann and Cremer (1999).

However, the benefit of SIM is not only the improved lateral resolution but also the improved axial optical sectioning resulting especially in an improved contrast compared to conventional wide-field microscopy. A theoretical analysis of the optical sectioning ability of SIM has been done by Karadaglić and Wilson (2008).

#### 2.1.2. The microscope

Most commonly used SIM microscopes use either a physical grating (Heintzmann and Cremer, 1999; Gustafsson, 2000), or a synthetic grating generated by a spatial light modulator (Hirvonen et al., 2008; Kner et al., 2009) in an intermediate image plane to create the modulated pattern in the object plane.

In this work, a different approach applying an interferometer configuration was used. This will be denoted as SIM<sub>HD</sub>.

The setup, built from custom-made elements, is based on an inversely applied specially designed widefield (non-scanning) fluorescence microscope. The structured illumination in the object plane is generated by a Twyman-Green interferometer. A schematic of the setup is displayed in Fig. 2. The excitation laser beam ( $\lambda_{\text{exc}} = 404, 488, 568, 647$  nm) is directed to a 50% beam splitting cube (Fig. 2, cube A), positioned in a focal point of the focusing lens. Half of the beam is reflected by  $90^\circ$  as the other half passes through the cube without change of direction. The resulting two beams are then reflected with mirrors by  $180^\circ$  back into the cube. After the light passes the beam splitter again, two beams, each at  $1/4$  intensity are generated, that leave the cube heading towards the focusing lens. As the two beams travel the same distance, they are coherent and generate an interference pattern. If the beam splitting cube is rotated around the axis perpendicular to the ground by an angle  $\theta$ , one beam is deflected by  $2\theta$ , as the other beam is deflected by  $-2\theta$ . Thus the interference pattern can be adjusted by rotating the beam splitter. The beams pass the focusing lens, and are then deflected by a dichromatic beam splitter (AHF Z488/568/647) by  $90^\circ$  towards the high numerical objective (Leica HCX PL APO 100x/1.4-0.7 OIL CS). After passing through the focusing lens and the objective, the interference of the two beams in the object plane generates a sinusoidal pattern with a modulation parallel to the object plane. The orientation of the modulation can be changed by rotating the beam splitter around an axis parallel to the ground and perpendicular to the previous rotation axis. It is therefore possible to generate sinusoidal interference patterns in the intermediate image plane with arbitrary period and direction, which makes it possible to adjust the period of the pattern in accordance with the particular task and wavelength. To control the generated pattern, a part of the exci-

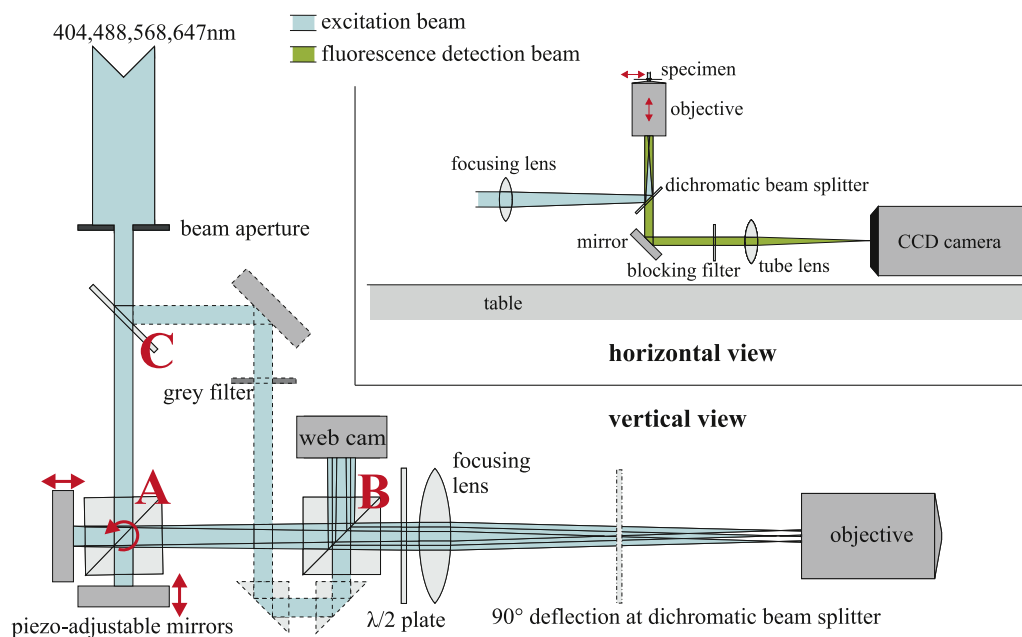


**Fig. 2.** Interferometer setup of the excitation beam. The schematic is simplified. The excitation beams are deflected by 90° onto the vertically applied objective by a dichromatic beam splitter. The deflection is not shown in the vertical view to improve the visibility. The detection path is also not shown in the vertical view as the interferometer is not shown in the horizontal view. The elements dashed are used for the optional three-beam-interference mode. The objects labeled with A, B and C are beam splitters. The arrows indicate movable elements.

tation intensity is reflected by a second beam splitter (B) onto a CCD-chip. The microscope also offers the option to use a third beam, not deflected by an angle and positioned central to the two outer deflected beams, in order to generate a three-beam interference pattern. The beam splitter extracting the central beam (C) is located in the beam line previous to the other beam splitters. The phase of the interference pattern can be altered by shifting the relative phases of the separate beams. To accomplish this accurately and quickly, piezo actuators are attached to the mirrors facing the rotatable beam splitting cube (A). The design of the microscope can also be used for Standing Wave Total Internal Reflection Fluorescence (SW-TIRF) microscopy. The emission light from the object is collected by the objective, and then passes through the dichromatic beam splitter through an additional blocking filter (AHF Z488/568/647M V2) and tube lens into the CCD-camera (PCO sensicam qe).

## 2.2. Sample preparation

The samples were provided by the Department of Ophthalmology, University of Heidelberg, Germany. Histological sections of the macular region of 68 and 89 years old patients were obtained. The enucleation of the eyes was conducted due to ophthalmologic indication. However, funduscopy and histological examination with light microscopy revealed no retinal or RPE abnormalities. The patients gave written informed consent for further scientific usage. Procedures followed the tenets of the Declaration of Helsinki.

The enucleated eyes were fixed with 4% paraformaldehyde in phosphate-buffered saline (PBS, pH 7.4) and embedded in paraffin. 4 μm thick histological sections of the macular region were prepared and fixed on microscope slides, de-paraffinized with xylene (3 × 5 min) and subsequently rehydrated through graded ethanol and stored in PBS. For further microscopic analysis, the slides were embedded with SlowFade Antifade (Invitrogen, Carlsbad, California, USA) and covered with cover slides.

To ensure imaging the macular region, a standard widefield fluorescence microscope (LEICA DMRB) was used to select regions of

interest that were subsequently labeled by markings on the back side of the slides.

## 2.3. Data acquisition and image processing

The previously selected regions in the specimen were analyzed with the SIM<sub>HD</sub> microscope with 488, 568 and 647 nm excitation consecutively. Even though, three beam interference (grid projection) is capable to perform better in theory (Karadaglić and Wilson, 2008), two beam interference (fringe projection) was used for two reasons: In the case of two beam interference, fewer images are necessary to reach a sufficiently high signal-to-noise ratio (SNR) reducing acquisition time and photo bleaching effects on the specimen. On the other hand, because of the axial modulation of the three beam interference pattern, the axial position has to be calibrated prior to the acquisition to achieve optimal results. This calibration has to be done for each illumination wavelength and grating orientation separately implying additional illumination of the specimen and a delay of the data acquisition process. For each of the three grating orientations, a series of 10 images was acquired with different phases of the sinusoidal intensity pattern. A total of three images per direction would have been sufficient to generate a high resolution image, but the count was raised to ten to increase the SNR. Hence a total of 30 raw images (total registration time ~3 s) was acquired to produce the data for one high resolution image. The grating spacing of the illumination pattern in the object plane was set to 275, 325 and 350 nm for the illumination wavelengths of 488, 568 and 647 nm, respectively, resulting in a lateral resolution improvement by a factor of roughly 1.7. The actual resolution is dependent on the emission spectrum. Using Abbe's resolution definition (Abbe, 1873), for 488 nm excitation and an emission wavelength of 553 nm (emission maximum of lipofuscin granules under 457.9 nm excitation (Haralampus-Grynawski et al., 2003), the calculated lateral resolution is 115 nm. With these values, a good optical sectioning is ensured while also attaining significant resolution improvement.

After computational reconstruction of the SIM images for the three different excitation wavelengths, color coded images were

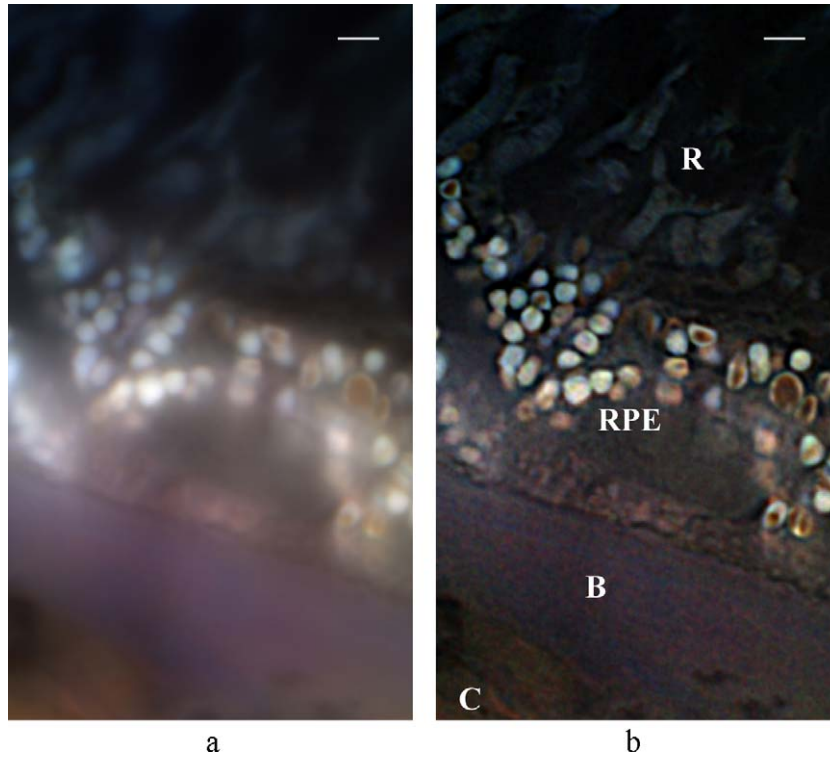


**Fig. 3.** Overview image. The SIM image (b) shows more details and less out of focus light than the widefield image (a). The background of each channel is subtracted and each channel is stretched to full dynamic range. The Bruch membrane (B) is located between the choroid (C) and the retinal pigment epithelium (RPE). On the top of the image endings of retinal rod cells (R) can be seen. The scale bar is 2  $\mu\text{m}$ .

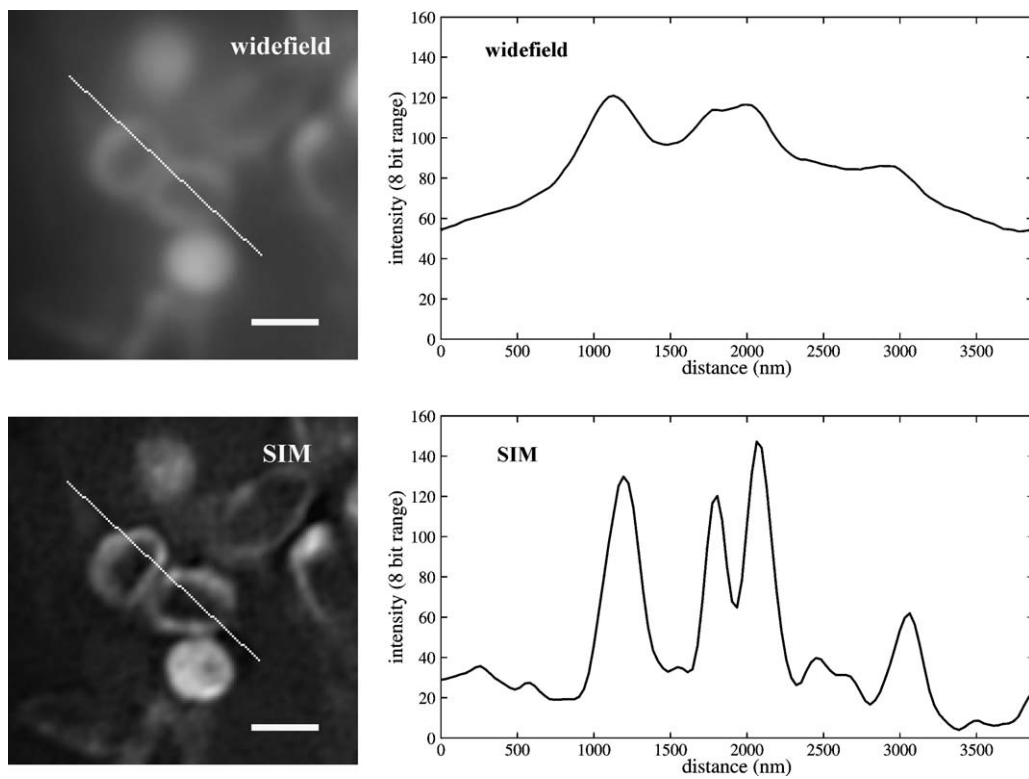


**Fig. 4.** Resolution improvement. To visualize the improvement in contrast and in resolution, the intensity (gray value) along a line (thin tilted line) in both widefield and structured illumination image is plotted. The intensity of both images is normalized to full dynamic range. The background intensity is respectively set to zero. The specimen was excited with 488 nm wavelength. The scale bar is 1  $\mu\text{m}$ .

generated to better distinguish spectral variances in the fluorescence response. For that purpose the background of the single images was subtracted independently and the images were each stretched to full dynamic range. Subsequently they were joined coded as separate channels of a three color RGB image. Hence the red channel corresponds to 647 nm excitation, the green channel to 568 nm and the blue channel to 488 nm excitation.

### 3. Results

When comparing the acquired SIM images with the standard widefield (non-scanning) data, a considerable improvement is apparent (Figs. 3 and 4). Not only the contrast is greatly improved, but also the optical resolution is enhanced by an estimated factor of 1.6–1.7 depending on the wavelength. Thus, previously irresolvable details can be discovered.

As lipofuscin has a broad fluorescence in the visible spectrum (Haralampus-Grynaviski et al., 2003), fluorescence of lipofuscin can be excited with all used wavelengths. However, emission response was strongest for 488 and 568 nm excitation.

In Fig. 3b it is visible, that the single lipofuscin granules are shaded in different colors, showing that the fluorescence spectrum varies between different granules in one cell.

Fig. 4 shows the intensity along a line through structures in RPE cells under 488 nm excitation each in a widefield image and the corresponding structured illumination image. The gray value (intensity) of both images was normalized to full 8 bit range and the background intensity was subtracted.

The improvement of contrast in the SIM image is apparent by the efficient suppression of out of focus light resulting in improved optical sectioning that can be seen in the higher dynamic in the examined region. The lateral resolution enhancement allows additional details to be seen (e.g. the two circular structures in the center of the image can clearly be separated in the SIM image).

However, because the analyzed specimen exhibits very strong out-of-focus fluorescence, the improvement of optical sectioning is more important for the visible enhancement in the images than the lateral resolution improvement.

### 4. Discussion

The structured illumination microscopy applied in this work was capable to resolve the fluorescent distribution of the small autofluorescent structures in RPE tissue sections for three different excitation wavelengths (488, 568, 647 nm).

Another remarkable information in the acquired images is the fact, that the excitation spectrum of single lipofuscin granules in the cell appears to be different.

Lipofuscin in RPE cells has been the subject of several previous researches because the pigment is believed to play a role in pathogenesis in different retinal diseases, predominantly in age related macular degeneration. To gather high resolution structural information, in these studies predominantly electron microscopy (e.g. Feeney, 1978), but also the super resolution optical method of two-photon-excited fluorescence (TPEF) (e.g. Bindewald-Wittich et al., 2006) was used.

In the work of Bindewald-Wittich et al. (2006), one-photon confocal laser scanning microscopy (CLSM) and two-photon-excited fluorescence (TPEF) with a CLSM setup was used to analyze the RPE specimen. The autofluorophore distribution in the RPE is rather difficult to acquire with light microscopy in high resolution, because the in focus signal is relatively weak while the out focus signal is strong. This results in a low signal-to-noise ratio (SNR) in conventional widefield microscopy and conventional CLSM. To increase the SNR in CLSM, the detection pinhole has to be adjusted to a

large diameter which results in a relatively poor suppression of out of focus information and resolving power. Thus, in the papers of Bindewald-Wittich et al. (2006), La Schiazza and Bille (2008) and related publications, the benefits of two-photon over one-photon confocal microscopy are described. As TPEF excites predominantly in the focus region, this technique is capable to suppress out of focus information very effectively even with the confocal's detection pinhole widely open. However, because of the high wavelength of the infrared excitation beam in TPEF, the lateral resolution improvement of the utilized confocal microscope can only be marginal (Bindewald-Wittich et al. (2006) quote the lateral resolution to be roughly 200 nm).

In contrast to confocal microscopy methods, SIM uses a wide-field detection, where no fluorescence light is blocked intentionally by apertures. Because of this procedure, much less in-focus light is lost resulting in a higher SNR. In SIM, the out-of-focus information contained in the acquired data can be separated afterwards in the reconstruction process of the final images from the raw data.

Because the resolution improvement and the optical sectioning happen after the image acquisition, the widefield imaging process itself is simpler than in confocal microscopy where the observed spot is scanned over the focal region during imaging.

In the results presented here we show that SIM is a competitive method to analyze fluorescent structures in RPE cells providing an unmatched lateral resolution down to 115 nm (calculated value for the highest object distance information that can be resolved (Abbe, 1873)). In contrast to many other super resolution techniques that require certain specifications for the fluorophore or the embedding media used, SIM can be applied whenever normal widefield fluorescence microscopy can be used.

The interferometer setup of the microscope exhibits a great variability and is therefore easy to adjust to different excitation wavelengths in contrast to a solid grid SIM setup.

The fact that SIM performs well in this autofluorescence study, encourages further applications and researches, such as implementing SIM to examine living tissue in vitro or even in vivo.

### Acknowledgements

The support of the University of Heidelberg, of the Deutsche Forschungsgemeinschaft (SPP1 128); and of the European Union (In Vivo Molecular Imaging Consortium, [www.molimg.gr](http://www.molimg.gr)) to Christoph Cremer is gratefully acknowledged.

### References

- Abbe, E., 1873. Beitrage zur Theorie des Mikroskops und der mikroskopischen Wahrnehmung. *Archiv für Mikroskopische Anatomie* 9, 413–420.
- Bindewald-Wittich, A., Han, M., Schmitz-Valckenberg, S., Snyder, S.R., Giese, G., Bille, J.F., Holz, F.G., 2006. Two-photon-excited fluorescence imaging of human RPE cells with a femtosecond Ti:sapphire laser. *Investig. Ophthalmol. Vis. Sci.* 47 (10), 4553–4557.
- Cremer, C., Cremer, T., 1978. Considerations on a laser-scanning-microscope with high resolution and depth of field. *Microsc. Acta* 81, 31–44.
- Cremer, C., von Ketteler, A., Lemmer, P., Kaufmann, R., Weiland, Y., Mueller, P., Hausmann, M., Baddeley, D., Amberger, R., 2010. Far-field fluorescence microscopy of cellular structures at molecular optical resolution. In: Diaspro, A. (Ed.), *Nanoscopy and Multidimensional Optical Fluorescence Microscopy*. Taylor & Francis.
- Eldred, G.E., Katz, M.L., 1988. Fluorophores of the human retinal pigment epithelium: separation and spectral characterization. *Exp. Eye Res.* 47, 71–86.
- Feeney, L., 1978. Lipofuscin and melanin of human retinal pigment epithelium. Fluorescence, enzyme cytochemical, and ultrastructural studies. *Investig. Ophthalmol. Vis. Sci.* 17, 583–600.
- Gustafsson, M.G.L., 2000. Surpassing the lateral resolution limit by a factor of two using structured illumination microscopy. *J. Microsc.* 198 (2), 82–87.
- Haralampus-Grynaviski, N.M., Lamb, L.E., Clancy, C.M.R., Skumatz, C., Burke, J.M., Sarna, T., Simon, J.D., 2003. Spectroscopic and morphological studies of human retinal lipofuscin granules. *Proc. Natl. Acad. Sci. U.S.A.* 100, 3179–3184.
- Heintzmann, R., Cremer, C.G., 1999. Laterally modulated excitation microscopy: improvement of resolution by using a diffraction grating. *Proc. SPIE* 3568, 185–196.

- Hell, S., Stelzer, E.H.K., 1992. Properties of a 4Pi confocal fluorescence microscope. *J. Opt. Soc. Am. A* 9, 2159–2166.
- Hell, S.W., Wichmann, J., 1994. Breaking the diffraction resolution limit by stimulated emission: stimulated-emission-depletion fluorescence microscopy. *Opt. Lett.* 19, 780–782.
- Hirvonen, L., Mandula, O., Wicker, K., Heintzmann, R., 2008. Structured illumination microscopy using photoswitchable fluorescent proteins. *Proc. SPIE* 6861, 68610L.
- Karadaglić, D., Wilson, T., 2008. Image formation in structured illumination wide-field fluorescence microscopy. *Micron* 39 (7), 808–818.
- Kner, P., Chhun, B.B., Griffis, E.R., Winoto, L., Gustafsson, M.G.L., 2009. Super-resolution video microscopy of live cells by structured illumination. *Nat. Methods* 6, 339–342.
- La Schiazza, O., Bille, J.F., 2008. High-speed two-photon excited autofluorescence imaging of ex vivo human retinal pigment epithelial cells toward age-related macular degeneration diagnostic. *J. Biomed. Opt.* 13, 064008.
- Ng, K.P., Gugu, B., Renganathan, K., Davies, M.W., Gu, X., Crabb, J.S., Kim, S.R., Rozanowska, M.B., Bonilha, V.L., Rayborn, M.E., et al., 2008. Retinal pigment epithelium lipofuscin proteomics. *Mol. Cell. Proteomics* 7, 1397–1405.
- Rayleigh, L., 1896. On the theory of optical images, with special reference to the microscope. *Philos. Mag.* 42, 167–195.
- Sparrow, J.R., Nakanishi, K., Parish, C.A., 2000. The lipofuscin fluorophore A2E mediates blue light-induced damage to retinal pigmented epithelial cells. *Investig. Ophthalmol. Vis. Sci.* 41, 1981–1989.